

## IMMUNOBIOLOGY

## Polygenic mutations in the cytotoxicity pathway increase susceptibility to develop HLH immunopathology in mice

Fernando E. Sepulveda,<sup>1,2</sup> Alexandrine Garrigue,<sup>1,2</sup> Sophia Maschalidi,<sup>1,2</sup> Meriem Garfa-Traore,<sup>3</sup> Gaël Ménasché,<sup>1,2</sup> Alain Fischer,<sup>1,2,4,5</sup> and Geneviève de Saint Basile<sup>1,2,6</sup>

<sup>1</sup>INSERM Unité Mixte de Recherche 1163, Laboratory of Normal and Pathological Homeostasis of the Immune System, Paris, France; <sup>2</sup>Paris Descartes University-Sorbonne Paris Cité, Imagine Institute, Paris, France; <sup>3</sup>Cell Imaging Platform, INSERM US24 Centre National de la Recherche Scientifique Unité Mixte de Service 3633, Structure Fédérative de Recherche Necker, Paris Descartes Sorbonne Paris Cité University, Paris, France; <sup>4</sup>Immunology and Pediatric Hematology Department, Necker Children's Hospital, Assistance Publique-Hôpitaux de Paris, Paris, France; <sup>5</sup>Collège de France, Paris, France; and <sup>6</sup>Centre d'Etudes des Déficiences Immunitaires, Assistance Publique-Hôpitaux de Paris, Hôpital Necker, Paris, France

## Key Points

- The accumulation of monoallelic mutations in HLH-causing genes impairs lymphocyte cytotoxicity contributing to HLH immunopathology in mice.
- A polygenic model may account for some of the cases of secondary HLH observed in humans.

**Hemophagocytic lymphohistiocytosis (HLH) is a life-threatening hyperinflammatory disease. Inherited forms of HLH are caused by biallelic mutations in several effectors of granule-dependent lymphocyte-mediated cytotoxicity. A small proportion of patients with a so-called "secondary" form of HLH, which develops in the aftermath of infection, autoimmunity, or cancer, carry a monoallelic mutation in one or more HLH-associated genes. Although this observation suggests that HLH may have a polygenic mode of inheritance, the latter is very difficult to prove in humans. In order to determine whether the accumulation of partial genetic defects in lymphocyte-mediated cytotoxicity can contribute to the development of HLH, we generated mice that were doubly or triply heterozygous for mutations in HLH-associated genes, those coding for perforin, Rab27a, and syntaxin-11. We found that the accumulation of monoallelic mutations did indeed increase the risk of developing HLH immunopathology after lymphocytic choriomeningitis virus infection. In mechanistic terms, the accumulation of heterozygous mutations in the two degranulation genes Rab27a and syntaxin-11, impaired the dynamics and secretion of cytotoxic granules**

**at the immune synapse of T lymphocytes. In addition, the accumulation of heterozygous mutations within the three genes impaired natural killer lymphocyte cytotoxicity in vivo. The genetic defects can be ranked in terms of the severity of the resulting HLH manifestations. Our results form the basis of a polygenic model of the occurrence of secondary HLH. (*Blood*. 2016;127(17):2113-2121)**

## Introduction

Hemophagocytic lymphohistiocytosis (HLH) is a rare, life-threatening syndrome, characterized by severe hyperinflammation and immunopathologic processes in several tissues. These features result from organ infiltration by over-activated CD8 T cells and macrophages, which produce high levels of cytokines such as interferon (IFN)- $\gamma$ , tumor necrosis factor (TNF)- $\alpha$ , interleukin (IL)-6, and IL-18.<sup>1-3</sup> Consequently, patients with HLH develop prolonged fever, hepatosplenomegaly, pancytopenia, liver failure and, in many cases, central neurologic manifestations. This disease can affect both children and adults, and cases can be broadly classified as "primary" or inherited and "secondary" HLH with no hint for an inherited cause.<sup>4,5</sup> Primary HLH predominates in early childhood, and has a clearly autosomal recessive pattern of inheritance caused by genetic defects in the perforin-dependent granule exocytosis pathway of cytotoxic lymphocytes. Biallelic mutations in the gene coding for perforin (ie, *PRF1*) are responsible for familial lymphohistiocytosis type 2 (FHL2),<sup>6</sup> with the involvement of the *UNC13-D* gene in FHL3,<sup>7</sup> *STX11* in FHL4,<sup>8</sup> *STXB2* in FHL5,<sup>9,10</sup> *RAB27A* in Griscelli syndrome

type 2,<sup>11</sup> and *LYST* in Chediak-Higashi syndrome.<sup>12,13</sup> Furthermore, signaling lymphocytic activation molecule-associated protein deficiency in X-linked lymphoproliferative type 1 syndrome also leads to HLH and defective cytotoxicity against B cells, frequently in the context of Epstein-Barr virus infection.<sup>14</sup>

Animal models of HLH, in which cytotoxicity-deficient mice are challenged with lymphocytic choriomeningitis virus (LCMV), have been invaluable for understanding the pathogenesis of HLH under defined conditions. Following LCMV infection, genetically modified mice lacking cytotoxic effectors (such as *Prf1*, *Rab27a*, *Unc13d*, *Stx11*, and *Lyst* mice) recapitulate most of the features of HLH following LCMV infection.<sup>15-20</sup> These include severe leukopenia, anemia, and hypercytokinemia (mainly involving IFN- $\gamma$  and inflammatory cytokines), elevated liver enzymes levels, splenomegaly, and tissue infiltration by activated macrophages that can be fatal. In *Prf1*-deficient mice, the HLH-like phenotype is thought to result from the failure of the cytotoxic cell to kill and eliminate the infected and antigen presenting

Submitted December 21, 2015; accepted February 6, 2016. Prepublished online as *Blood* First Edition paper, February 10, 2016; DOI 10.1182/blood-2015-12-688960.

The online version of this article contains a data supplement.

There is an Inside *Blood* Commentary on this article in this issue.

The publication costs of this article were defrayed in part by page charge payment. Therefore, and solely to indicate this fact, this article is hereby marked "advertisement" in accordance with 18 USC section 1734.

© 2016 by The American Society of Hematology

cells (APCs), an important feedback required to eliminate T-cell-mediated immune response.<sup>21,22</sup> In the absence of effective cytotoxicity, APCs continue to stimulate cytotoxic T lymphocytes (CTLs), whereas natural killer (NK) cell cytotoxicity fails to reduce T-cell activation.<sup>21,22</sup> In the various mutant mice, hyperactivated T cells secrete high levels of IFN- $\gamma$ , which appears to be critical for the development of HLH. Furthermore, the magnitude of cytotoxicity impairment appears to be the best predictor of the development and severity of HLH in mice, as shown by studies of the time course of HLH onset in various HLH-prone strains with defects in the granule-dependent cytotoxic pathway.<sup>20,23</sup> The same appears to be true in humans.<sup>20,23</sup>

The secondary forms of HLH generally occur later in life than the primary forms. The condition develops in response to infections, in association with concurrent malignancies or in the context of autoimmune or rheumatologic disorders.<sup>4</sup> However, the distinction between primary and secondary forms of HLH is becoming blurred. Biallelic hypomorphic mutations in HLH genes, which do not fully abolish cytotoxicity, are associated with late-onset of HLH in adults up to the age of 62 years.<sup>24-27</sup> Furthermore, adults with HLH have been found to carry a monoallelic mutation in one or more HLH-associated genes.<sup>26,28-30</sup> This observation prompted the hypothesis whereby, additive effects of monoallelic variants in genes encoding cytotoxic effector proteins may account for some cases of HLH. However, this hypothesis has yet to be demonstrated. Murine models of HLH constitute a powerful tool for addressing this question.

In the present study, we generated mice carrying heterozygous mutations in combinations of two to three HLH genes. The study's objective was to determine whether the accumulation of partial defects in lymphocyte cytotoxicity could lead to the development of HLH and the impairment of immune homeostasis. We found that when each of the tested components in the pathway, *Prf1*, *Rab27a*, and *Stx11* is present in a half-dose, a 2- or 3-gene combination reduces cytotoxic activity and increases the risk of HLH development. Our results support the existence of polygenic inheritance in secondary HLH.

## Methods

### Mice and mice studies

C57BL/6J wild-type (WT), C57BL/6J-*Prf1*<sup>tm1Sdz/J</sup> (*Prf1*<sup>-/-</sup>), C57BL/6J-*Rab27a*<sup>ash/J</sup> (*Rab27a*<sup>-/-</sup>), and C57BL/6J-*Stx11*<sup>-/-</sup> mice have been described previously.<sup>19,20,31</sup> Mice carrying monoallelic defects in HLH genes were generated by breeding the different knockout (KO) mice between them (see supplemental Methods, available on the *Blood* Web site). Mice were maintained in pathogen-free conditions and handled according to national and institutional guidelines. Based on animal care guidelines, mice had to be eliminated when they had lost >30% of their weight. Induction of HLH by LCMV infection and analysis of the clinical and biological parameters of HLH in mice were done as previously described,<sup>20,22</sup> and are detailed in supplemental Methods.

### In vitro CD8<sup>+</sup> T-cell activation and degranulation assay

Degranulation assay were performed on CD8<sup>+</sup> T cells purified from the spleen as previously reported<sup>20</sup> (see supplemental Methods).

### In vivo assay for NK cytotoxic activity

Spleen cell suspensions from  $\beta$ 2-microglobulin ( $\beta$ 2m)-deficient mice and C57BL/6 controls were differentially labeled with CellTrace carboxyfluorescein diacetate succinimidyl ester (CFSE) or Violet Cell Proliferation Kit according to the manufacturer's instructions (Thermo Fischer Scientific). The two populations were mixed at a 1:1 ratio and IV injected into recipient mice. Sixteen hours later, recipients were euthanized and spleen mononuclear cell (MNC) suspensions were analyzed for CFSE and Violet staining by flow cytometer. The cytotoxic index was

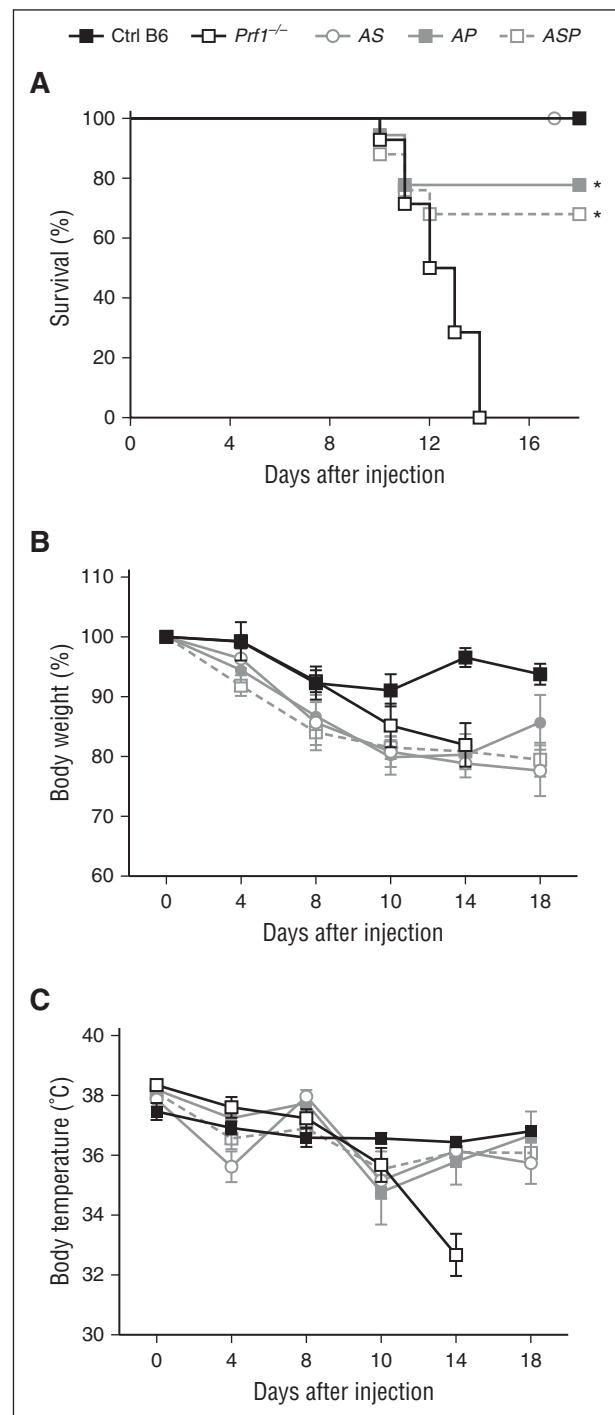
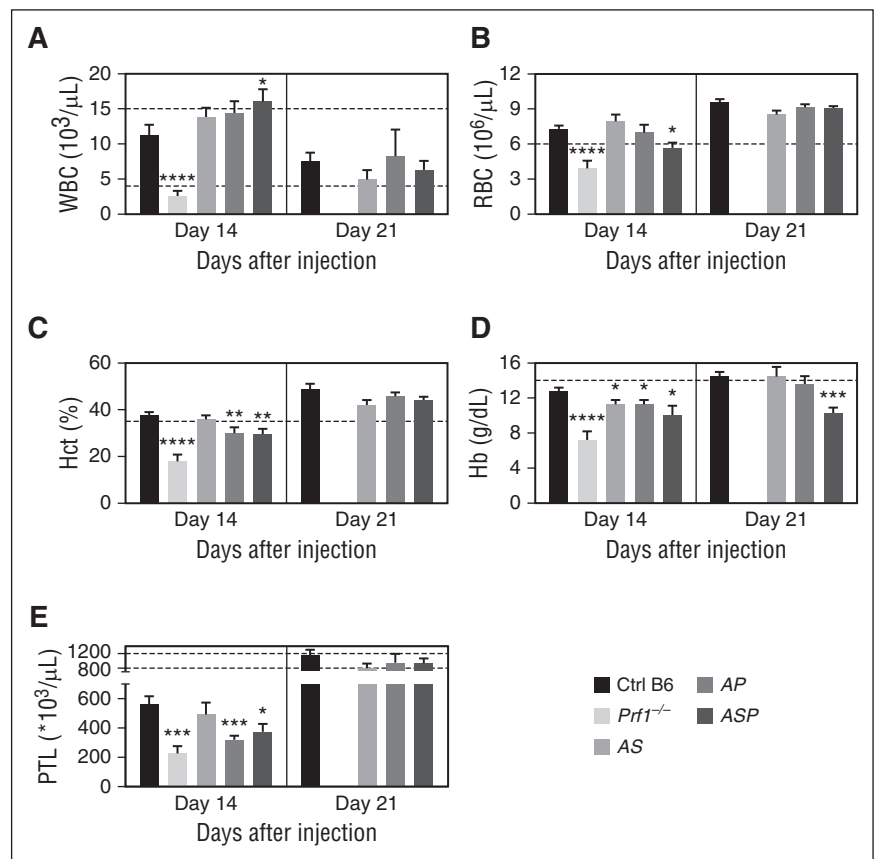


**Figure 1. Accumulation of monoallelic mutations in HLH-causing genes increases the risk to develop clinical manifestations of HLH.** Control (black squares), *Prf1*<sup>-/-</sup> (open squares), *Rab27a*<sup>+/+</sup> *Stx11*<sup>+/+</sup> (AS, open gray circles), *Rab27a*<sup>+/+</sup> *Prf1*<sup>+/+</sup> (AP, gray squares), and *Rab27a*<sup>+/+</sup> *Prf1*<sup>+/+</sup> *Stx11*<sup>+/+</sup> mice (ASP, gray open squares) were infected with 200 PFU of LCMV-WE. (A) Survival, (B) body weight, and (C) body temperature are shown. Data (mean  $\pm$  standard error of the mean [SEM]) are representative of 3 to 4 independent experiments with at least 3 mice in each group. \* $P < .05$ .

determined as the ratio of killing of control vs  $\beta$ 2m-deficient cells corrected by the ratio of cells present at the input. The values were corrected by subtracting the spontaneous cell lysis and reported to maximum cell lysis mediated by control cells.

Immunodetection of proteins were performed using standard techniques (see supplemental Methods). The intensity of the immunoblot bands was quantified using ImageJ Software and Gel-Pro Analyzer version 3.1.

**Figure 2. Poly heterozygous mice for HLH-causing genes display biological features of HLH upon LCMV infection.** Control (black bars), *Prf1*<sup>-/-</sup> (lightest gray bars), *Rab27a*<sup>+/-</sup> *Stx11*<sup>+/-</sup> (AS, light gray bars), *Rab27a*<sup>+/-</sup> *Prf1*<sup>+/-</sup> (AP, medium gray bars), and *Rab27a*<sup>+/-</sup> *Prf1*<sup>+/-</sup> *Stx11*<sup>+/-</sup> mice (ASP, dark gray bars) were infected with 200 PFU of LCMV-WE. (A) WBC counts, (B) RBC counts, (C) hematocrit, (D) Hb, and (E) platelets counts were monitored 14 and 21 days postinfection. Data (mean ± SEM) are representative of 3 to 4 independent experiments with at least 3 mice in each group. Dashed lines represent normal values for mice. \**P* < .05; \*\**P* < .01; \*\*\**P* < .001; \*\*\*\**P* < .0001. Hct, hematocrit; PTL, platelets.



### Total internal reflection fluorescence (TIRF) microscopy

To perform TIRF assays, CTL were labeled with 2 μg/mL of wheat germ agglutinin (WGA)-Alexa555 (Molecular Probes) for 20 minutes at 37°C, and then incubated for 16 hours with 1000 U/mL of IL-2.<sup>32</sup> Glass coverslips coated with anti-CD3 antibody were used to stimulate WGA-labeled CTL (3 × 10<sup>5</sup> per well). After the cells had attached to the glass, a TIRF image was acquired for 5 minutes (exposure time, 200 milliseconds). During the observation, the cells were kept at 37°C. Fluorescence data were acquired with an Eclipse Ti-E TIRF imaging system (Nikon). Images were acquired with a Roper Scientific QuantEM 512 SC camera (Nikon) and NIS-Elements Advanced Research software (version 3.1). Image sets were processed with ImageJ and Imaris software and analyzed blinded.

### Statistical analysis

Data were analyzed with GraphPad Prism 4 software. Survival and HLH incidence curves were analyzed by using the log-rank test. All other analyses were performed by using Student *t* tests or one-way analysis of variance with posttest. Differences were considered to be statistically significant when *P* < .05 (indicated as \**P* < .05, \*\**P* < .01, \*\*\**P* < .001, and \*\*\*\**P* < .0001).

## Results

### In mice, the accumulation of monoallelic mutations in HLH genes induces manifestations of HLH

Both others and our study group have previously shown that following LCMV infection, mice that are heterozygous for a single HLH gene (ie, *Rab27*<sup>+/-</sup> or *Stx11*<sup>+/-</sup> animals) do not display the features of HLH when compared with WT mice.<sup>18,19,31</sup> The same is true for *Prf1*<sup>+/-</sup> mice (supplemental Figure 1). To evaluate the impact of an accumulation

of monoallelic mutations along the granule-dependent cytotoxicity pathway, we generated C57BL/6J (B6) mice carrying heterozygous mutations in several HLH genes. By breeding perforin- (*Prf1*<sup>-/-</sup>), Ashen- (*Rab27a*<sup>-/-</sup>), and syntaxin-11-deficient (*Stx11*<sup>-/-</sup>) mice, we generated *Rab27a*<sup>+/-</sup> *Stx11*<sup>+/-</sup> mice (hereafter referred to as “AS mice”, for “Ashen syntaxin-11”), *Rab27a*<sup>+/-</sup> *Prf1*<sup>+/-</sup> mice (“AP mice”), and *Rab27a*<sup>+/-</sup> *Prf1*<sup>+/-</sup> *Stx11*<sup>+/-</sup> mice (“ASP mice”). In each of these strains, the monoallelic mutation results in half the normal level of protein expression (supplemental Figure 2). When compared with control (WT) B6 mice, heterozygous mice grew and developed normally and had normal immune cell distribution (T, B, NK cells, and APCs) in lymph nodes, thymus, and spleen (data not shown).

To determine the impact of the accumulation of monoallelic mutations in HLH genes on immune homeostasis and susceptibility to HLH, mice were infected with a single intraperitoneal injection of 200 plaque-forming units (PFUs) of LCMV-WE. As expected, control B6 mice survived the LCMV infection, whereas HLH progression in the cytotoxicity-deficient *Prf1*<sup>-/-</sup> mice was fatal about 2 weeks postinfection (Figure 1A), and mice had to be eliminated due to animal care guidelines. As previously reported,<sup>18,20,31,33</sup> the increased susceptibility in *Prf1*<sup>-/-</sup> mice was associated with body weight loss and a marked drop in body temperature (Figure 1B-C). The combination of monoallelic mutations in AS mice did not affect survival (Figure 1A). In contrast, the combinations of heterozygous mutations present in AP and ASP mice increased susceptibility to LCMV infection, because 20% to 30% of the mice in each group died around 10 days postinfection (Figure 1A). Compared with control B6 mice, the accumulation of monoallelic mutations in HLH genes led to sustained body weight loss following infection (Figure 1B), whereas the body temperature normalized rapidly in surviving mice (Figure 1C).

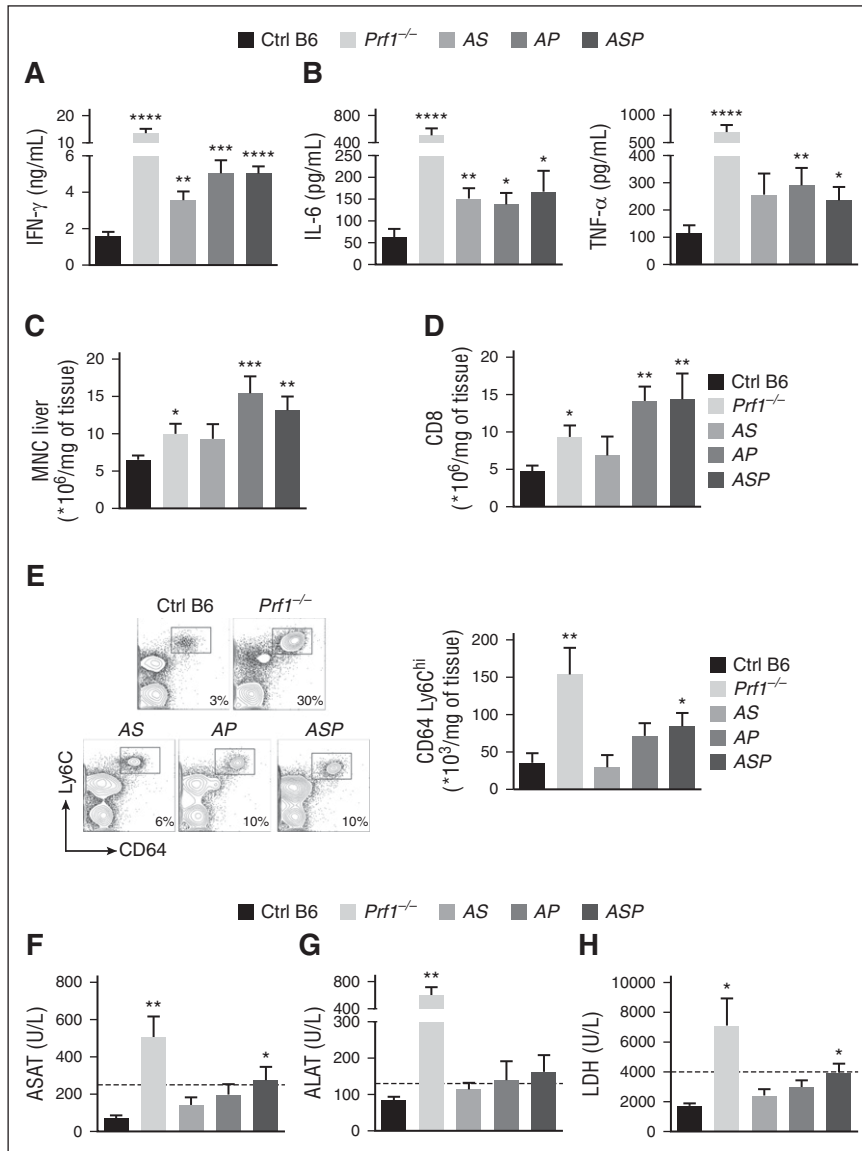


**Figure 3. Accumulation of heterozygous mutations in HLH-causing genes induces biological parameters of HLH after LCMV infection.** Control (black bars), *Prfl1*<sup>-/-</sup> (lightest gray bars), *Rab27a*<sup>+/-</sup> *Stx11*<sup>+/-</sup> (AS, light gray bars), *Rab27a*<sup>+/-</sup> *Prfl1*<sup>+/-</sup> (AP, medium gray bars), and *Rab27a*<sup>+/-</sup> *Prfl1*<sup>+/-</sup> *Stx11*<sup>+/-</sup> mice (ASP, dark gray bars) were infected with 200 PFU of LCMV-WE. (A) Serum IFN-γ on day 8 postinfection. (B) Serum IL-6 (left) and TNF-α (right) on day 14 postinfection. (C) MNC infiltration in liver on day 14 postinfection. (D) The percentage of CD8<sup>+</sup> among all MNCs from the liver. (E) Fluorescence-activated cell sorter (FACS) analysis of MNCs from liver cells gated on CD3<sup>-</sup> CD19<sup>-</sup> NK1.1<sup>-</sup> (left). Quantification of absolute numbers of CD64<sup>+</sup> Ly6C<sup>+</sup> in liver on day 14 postinfection (right). (F) ASAT on day 14 postinfection. (G) ALAT on day 14 postinfection. (H) Serum LDH on day 14 postinfection. Data (mean ± SEM) are representative of 3 to 4 independent experiments with at least 3 mice in each group. \**P* < .05; \*\**P* < .01; \*\*\**P* < .001; \*\*\*\**P* < .0001. ALAT, serum alanine aminotransferase; ASAT, serum aspartate aminotransferase; LDH, lactate dehydrogenase.

In homozygous cytotoxic-deficient *Prfl1*<sup>-/-</sup> mice, LCMV-induced HLH is characterized by severe pancytopenia (ie, low counts of white blood cells (WBCs), red blood cells (RBCs), and platelets; Figure 2). In contrast, LCMV infection of heterozygous mice was associated with leukocytosis, 2 weeks postinfection. This leukocytosis was statistically significant, relative to control mice, in the triple-heterozygote ASP mice (Figure 2A), and resulted mainly from an increase in the number of circulating, activated (CD44<sup>hi</sup> Ly6C<sup>hi</sup> KLRG1<sup>+</sup>) T lymphocytes (data not shown). The leukocytosis was only transient, because normal WBC counts were observed in all heterozygous mice 3 weeks postinfection (Figure 2A).

Relative to control mice, doubly heterozygous AS mice did not develop anemia 2 weeks postinfection (Figure 2B-D). Anemia was defined as significant impairment of at least two parameters among RBC counts, hematocrit, and hemoglobin (Hb) levels. In contrast, both AP and ASP mice developed anemia (Figure 2B-D). LCMV infection was also associated with thrombocytopenia in all heterozygous mice 2 weeks postinfection (Figure 2E). As was observed for the WBC counts, the changes in blood parameters seen in heterozygous mice were mostly transient and normalized over time. In fact, only the Hb level was still

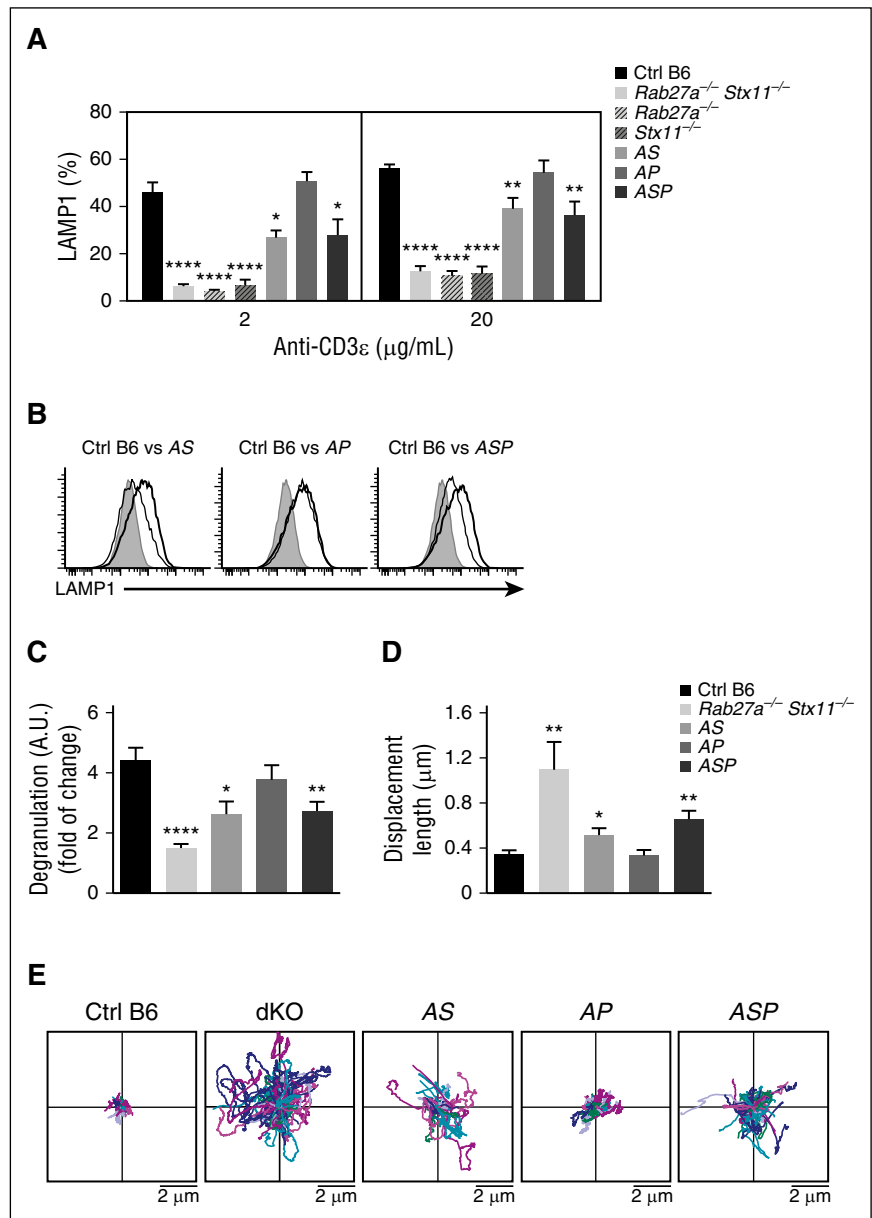
abnormally low in triply heterozygous ASP mice 21 days postinfection (Figure 2D).

These data show that the accumulation of monoallelic defects in HLH genes in mice is associated with (1) the transient development of clinical manifestations of HLH after viral infection, and (2) a fatal outcome in a small proportion of animals, with the mildest phenotype seen in AS mice.

### The severity of the biological features of HLH increases with the cumulative introduction of monoallelic mutations in HLH genes

To establish whether LCMV infection of doubly or triply heterozygous mice induced additional features of HLH, we measured several biological parameters in control, *Prfl1*<sup>-/-</sup>, and heterozygous mice. As expected, *Prfl1*<sup>-/-</sup> mice had high serum levels of IFN-γ and the inflammatory cytokines IL-6 and TNF-α after LCMV infection (Figure 3A-B). Similarly, doubly and triply heterozygous mice had high serum levels of IFN-γ (Figure 3A), although the increase was less pronounced than in *Prfl1*<sup>-/-</sup> mice (particularly for AS mice) (Figure 3A). Heterozygous mice still displayed elevated serum levels of IL-6 and TNF-α 2 weeks postinfection (Figure 3B), albeit to a lesser extent than *Prfl1*<sup>-/-</sup> mice.

**Figure 4. Accumulation of monoallelic mutations in HLH-causing genes impairs degranulation capacity and lytic granules' dynamics at the immune synapse.** Spleen CD8 T cells from control (black bars), *Rab27a*<sup>-/-</sup> *Stx11*<sup>-/-</sup> (lightest gray bars), *Rab27a*<sup>-/-</sup> (light gray dashed bars), *Stx11*<sup>-/-</sup> (dark gray dashed bars), *Rab27a*<sup>+/-</sup> *Stx11*<sup>+/-</sup> (AS, light gray bars), *Rab27a*<sup>+/-</sup> *Prf1*<sup>+/-</sup> (AP, medium gray bars), and *Rab27a*<sup>+/-</sup> *Prf1*<sup>+/-</sup> *Stx11*<sup>+/-</sup> mice (ASP, dark gray bars) were activated in vitro. Degranulation capacity was assessed upon re-stimulation with anti-CD3 antibody after 5 days of culture. (A) Graphs show the mean ± SEM of the percentage of LAMP1<sup>+</sup> cells at 2 doses of anti-CD3 (2 and 20 μg/mL). (B) A representative FACS analysis for degranulation of CD8 T cells from control (black histogram) and *Rab27a*<sup>-/-</sup> *Stx11*<sup>-/-</sup> (dashed histogram) cells vs *Rab27a*<sup>+/-</sup> *Stx11*<sup>+/-</sup> cells (gray histogram, left); *Rab27a*<sup>+/-</sup> *Prf1*<sup>+/-</sup> cells (gray histogram, middle); and *Rab27a*<sup>+/-</sup> *Prf1*<sup>+/-</sup> *Stx11*<sup>+/-</sup> cells (gray histogram, right). (C) Graphs show the mean ± SEM of LAMP1 variation on CD8 T cells from control (black bars), *Rab27a*<sup>-/-</sup> *Stx11*<sup>-/-</sup> (lightest gray bars), *Rab27a*<sup>+/-</sup> *Stx11*<sup>+/-</sup> (AS, light gray bars), *Rab27a*<sup>+/-</sup> *Prf1*<sup>+/-</sup> (AP, medium gray bars), and *Rab27a*<sup>+/-</sup> *Prf1*<sup>+/-</sup> *Stx11*<sup>+/-</sup> mice (ASP, dark gray bars). Data (mean ± SEM) are representative of 3 to 4 independent experiments. (D) TIRF analysis was performed on WGA A555-labeled activated CD8 T cells from control (black bars), *Rab27a*<sup>-/-</sup> *Stx11*<sup>-/-</sup> (lightest gray bars), *Rab27a*<sup>+/-</sup> *Stx11*<sup>+/-</sup> (AS, light gray bars), *Rab27a*<sup>+/-</sup> *Prf1*<sup>+/-</sup> (AP, medium gray bars), and *Rab27a*<sup>+/-</sup> *Prf1*<sup>+/-</sup> *Stx11*<sup>+/-</sup> mice (ASP, dark gray bars). TIRF analysis was performed in 5-minute acquisitions. Graphs show the mean ± SEM of length displacement. Data (mean ± SEM) are representative of 2 independent experiments with at least 10 cells per condition. (E) Two dimensional representation of the lytic granule tracking within the TIRF zone of representative activated CD8 T cells from control (Ctrl B6), *Rab27a*<sup>-/-</sup> *Stx11*<sup>-/-</sup> (dKO), *Rab27a*<sup>+/-</sup> *Prf1*<sup>+/-</sup> (AP), *Rab27a*<sup>+/-</sup> *Stx11*<sup>+/-</sup> (AS), and *Rab27a*<sup>+/-</sup> *Prf1*<sup>+/-</sup> *Stx11*<sup>+/-</sup> mice (ASP), analyzed in (D). The starting point of each trajectory was translated to the origin of the plot. \**P* < .05; \*\**P* < .01; \*\*\**P* < .001; \*\*\*\**P* < .0001. A.U., arbitrary units.



One of the hallmarks of LCMV-induced HLH consists of liver infiltration and destruction by immune cells. The number of MNCs, and particularly CD8T lymphocytes, in the liver was higher in *Prf1*<sup>-/-</sup> mice than in control mice, and even higher in heterozygous AP and ASP mice (Figure 3C-D). In *Prf1*<sup>-/-</sup> mice, LCMV infection induced massive liver infiltration by activated macrophages, relative to controls, as evidenced by both relative and absolute cell counts (Figure 3E). Although levels of inflammatory macrophage infiltration in doubly heterozygous AS and AP mice were similar to that observed in control mice, higher levels were seen in triply heterozygous ASP mice, although lower than in *Prf1*<sup>-/-</sup> mice (Figure 3E). Two weeks after LCMV infection, liver damage, as evidenced by elevated serum levels of liver enzymes, was more severe in triply heterozygous ASP mice than in control, AS, and AP mice (Figure 3F-H). These data indicate that the accumulation of monoallelic mutations within the granule-dependent cytotoxicity pathway increases the risk of developing biological features of HLH, and the number and severity of the features vary as a function of the gene dosage.

**Polygenic heterozygous mutations within the cytotoxicity pathway partially impair granule-dependent cytotoxicity in lymphocytes**

To determine whether the development of LCMV-triggered HLH manifestations in doubly or triply heterozygous mice was correlated with partial defects in the granule-dependent cytotoxicity pathway, we compared the in vitro degranulation capacities of activated CTLs from control mice, doubly heterozygous mice (AS and AP), the triply heterozygous ASP mouse, and a completely cytotoxicity-deficient mouse. CTLs purified from the *Rab27a*<sup>-/-</sup> *Stx11*<sup>-/-</sup> double KO mouse were used as a model in which exocytosis was absent (as measured in a lysosomal-associated membrane protein [LAMP]1 assay). The magnitude of the degranulation defect was similar in *Rab27a*<sup>-/-</sup> *Stx11*<sup>-/-</sup> double KO mice, and *Rab27a*<sup>-/-</sup> and *Stx11*<sup>-/-</sup> single KO mice (Figure 4A). As expected, granule exocytosis was normal in *Prf1*<sup>-/-</sup> mice (data not shown).<sup>20</sup>

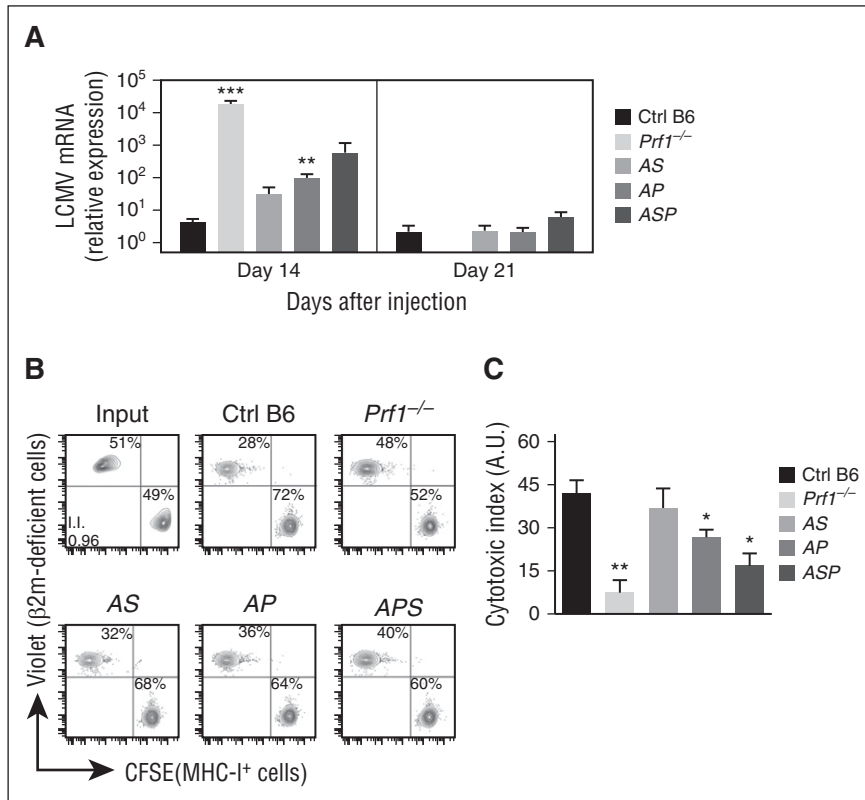


**Figure 5. Reduced cytotoxic activity of lymphocytes in mice carrying heterozygous mutations in several HLH-causing genes.** Control (black bars), *Prfl*<sup>-/-</sup> (lightest gray bars), *Rab27a*<sup>+/-</sup> *Stx11*<sup>+/-</sup> (AS, light gray bars), *Rab27a*<sup>+/-</sup> *Prfl*<sup>+/-</sup> (AP, medium gray bars), and *Rab27a*<sup>+/-</sup> *Prfl*<sup>+/-</sup> *Stx11*<sup>+/-</sup> mice (ASP, dark gray bars) were infected with 200 PFU of LCMV-WE. (A) LCMV titers in the liver of infected mice 14 and 21 days postinfection. Data (mean ± SEM) are representative of 3 to 4 independent experiments with at least 3 mice in each group. Control (black bars), *Prfl*<sup>-/-</sup> (lightest gray bars), *Rab27a*<sup>+/-</sup> *Stx11*<sup>+/-</sup> (AS, light gray bars), *Rab27a*<sup>+/-</sup> *Prfl*<sup>+/-</sup> (AP, medium gray bars), and *Rab27a*<sup>+/-</sup> *Prfl*<sup>+/-</sup> *Stx11*<sup>+/-</sup> mice (ASP, dark gray bars) were injected with a mix of control and β2-m-deficient spleen cells labeled with different fluorescent dyes (CFSE and Violet, respectively). Sixteen hours later, the presence of injected cells was quantified by FACS analysis. (B) FACS analysis of input cells (upper left) and MNCs from spleen of control (upper middle), *Prfl*<sup>-/-</sup> (upper right), *Rab27a*<sup>+/-</sup> *Stx11*<sup>+/-</sup> (AS, lower left), *Rab27a*<sup>+/-</sup> *Prfl*<sup>+/-</sup> (AP, lower middle), and *Rab27a*<sup>+/-</sup> *Prfl*<sup>+/-</sup> *Stx11*<sup>+/-</sup> mice (ASP, lower right panel). Data are representative of 2 independent experiments with at least 3 mice in each group. (C) Relative cytotoxic index. Data (mean ± SEM) are representative of 2 independent experiments. \**P* < .05; \*\**P* < .01; \*\*\**P* < .001. A.U., arbitrary units; MHC, major histocompatibility complex; mRNA, messenger RNA.

Compared with control CTLs, CD8 T cells from AS and ASP mice displayed an impairment in CD8 T-cell degranulation, albeit to a lesser extent than the KO mice (Figure 4A). These findings indicate the presence of residual granule secretion in the heterozygous mice. As expected, CD8 T cells from AP mice, which carry a monoallelic mutation in *Rab27a*, displayed normal degranulation (Figure 4A). Thus, monoallelic mutations in the cytotoxicity pathway do not significantly impair the exocytosis of lytic granules upon CTL activation *in vitro*; this observation correlates with the absence of HLH manifestations *in vivo* after LCMV infection. It is noteworthy that CD8 T cells from AS and ASP mice displayed a lower LAMP1 mean fluorescence intensity than control mice, suggesting a decrease in the number of lytic granules secreted per cell upon T-cell receptor activation (Figure 4B-C). The impaired degranulation of CD8 T cells from AS and ASP mice did not appear to be a consequence of impaired T-cell activation, because similar levels of activation markers (CD44 and CD62L) were simultaneously expressed in all cases (data not shown).

Given that a combination of monoallelic null mutations in *Rab27a* and *Stx11* partially impaired the exocytosis of lytic granules, we next sought to determine whether the impaired degranulation capacities in AS and ASP CD8 T cells were correlated with alterations in lytic granule dynamics at the immune synapse. To this end, we used TIRF microscopy to analyze and compare the behavior of lytic granules in CD8 T cells from WT mice, doubly heterozygous mice (AS and AP), triply heterozygous mice (ASP), and the *Rab27a*<sup>-/-</sup> *Stx11*<sup>-/-</sup> double KO mouse. The T cells were placed on anti-CD3-coated coverslips. A 16-hour pulse with fluorescent-labeled WGA specifically labeled the lytic granules and thus enabled their visualization with real-time video microscopy.<sup>32</sup> As expected, the vast majority of lytic granules from control CTL displayed a constrained movement in the TIRF area (Figure 4D-E). In contrast, most of the lytic granules from *Rab27a*<sup>-/-</sup>

*Stx11*<sup>-/-</sup> CD8 T cells were highly mobile, as evidenced by a greater mean displacement than controls (Figure 4D-E). These results indicate that the docking of lytic granules with the plasma membrane was defective, and agree well with previous reports on the regulatory roles of *Rab27a* (docking) and *Stx11* (tethering/fusion) in late degranulation.<sup>1</sup> The accumulation of monoallelic mutations in *Rab27a* and *Stx11* (in AS and ASP mice) partially impaired the docking of lytic granules with the plasma membrane, because the mean displacement was greater than for control cells but lower than for *Rab27a*<sup>-/-</sup> *Stx11*<sup>-/-</sup> cells (Figure 4D-E). The presence of a monoallelic mutation in *Prfl* had no additional effect. These *in vitro* results show that the accumulation of monoallelic mutations in *Rab27a* and *Stx11* impair lytic granule dynamics and degranulation in activated CTLs.

To determine whether the transient development of HLH manifestations observed in doubly and triply heterozygous mice (Figures 1-3) were indeed correlated with defective *in vivo* cytotoxicity, we indirectly evaluated cytotoxic effector function in CD8 by measuring LCMV viral titers in the liver 14 and 21 days postinfection. Indeed, as previously shown, CTLs play a key role in LCMV clearance.<sup>22,34</sup> Whereas control B6 mice were able to fully control LCMV replication, *Prfl*<sup>-/-</sup> mice were unable to clear the virus and had high LCMV titers 14 days postinfection (Figure 5A). Compared with control mice, doubly heterozygous mice (AS and AP) and triply heterozygous mice (ASP) cleared the virus more slowly (Figure 5A), suggesting that the accumulation of monoallelic mutations in HLH genes partially impairs CTL cytotoxic activity and delays viral clearance.

Recently, both others and our study group highlighted an immunoregulatory role for NK cytotoxicity in restraining CTL hyperactivation and preventing HLH immunopathology.<sup>22,35,36</sup> To determine whether the accumulation of heterozygous mutations in HLH genes impaired NK cytotoxicity *in vivo*, we assessed

NK-cell–dependent cytotoxicity against  $\beta 2m$ -deficient cells. To this end, we differentially labeled control and  $\beta 2m$ -deficient splenocytes with two fluorescent dyes and transferred them to control mice, doubly heterozygous mice (AS and AP), triply heterozygous mice (ASP), and a completely cytotoxicity-deficient *Prfl*<sup>-/-</sup> mouse. Sixteen hours later, we quantified the presence of control and  $\beta 2m$ -deficient splenocytes in the spleen. In AS, AP, and ASP mice, we observed a gradient of NK cytotoxic impairment, ranging from the absence of an impairment relative to controls (in AS mice) to a severe defect (in ASP mice) (Figure 5B-C). These results show that the accumulation of monoallelic mutations in HLH genes reduces the cytotoxic activity of both CTLs and NK cells, in strong correlation with the development of HLH manifestations. Taken as a whole, our data suggest that a minimum threshold of lymphocyte cytotoxicity is required to maintain immune homeostasis and prevent the onset of HLH immunopathology.

## Discussion

In humans with HLH, the cytotoxicity defect resulting from biallelic disruptive mutations in one of the HLH-related genes leads to a similar full-blown syndrome, although the distribution of ages at HLH onset differs significantly according to the affected gene.<sup>20,23</sup> The clinical and functional impact of cumulative monoallelic mutations in these genes has not been well characterized. This question is becoming particularly important, given the growing number of sporadic and adult cases of HLH carrying heterozygous mutations in one or several of the HLH-related genes.<sup>37,38</sup> The present results demonstrate that in well-defined murine models, the accumulation of partial genetic defects in the granule-dependent cytotoxicity pathway increases the likelihood of developing HLH.

Most of the manifestations that characterize full-blown HLH in homozygous, cytotoxic-deficient mutant mice, were observed in the triply heterozygous ASP mutant. However, in ASP mice, these manifestations were less severe than in homozygous, perforin-deficient mice and were transient in the surviving mice, but nevertheless were typical features of murine HLH. Double heterozygotes for *Rab27a*<sup>+/-</sup> and *Prfl*<sup>+/-</sup> (AP mice) or for *Rab27a*<sup>+/-</sup> and *Stx11*<sup>+/-</sup> (AS mice) displayed intermediate HLH patterns, although the features of HLH were more numerous and more intense in AP mice than in AS mice. Hence, in contrast to singly heterozygous *Rab27a*<sup>+/-</sup>, *Stx11*<sup>+/-</sup>, or *Prfl*<sup>+/-</sup> mice, which have the same phenotype as WT mice, partial defects in effectors of lymphocyte cytotoxic activity had cumulative effects on the development of HLH with an ordered hierarchy (*Rab27a*<sup>+/-</sup> *Stx11*<sup>+/-</sup> *Prfl*<sup>+/-</sup> (ASP) > *Rab27a*<sup>+/-</sup> *Prfl*<sup>+/-</sup> (AP) > *Rab27a*<sup>+/-</sup> *Stx11*<sup>+/-</sup> (AS) > *Rab27a*<sup>+/-</sup>, or *Stx11*<sup>+/-</sup> or *Prfl*<sup>+/-</sup> or WT). The observation that HLH was more severe in AP mice than in AS mice fits well with the relative severity previously reported for homozygous perforin vs syntaxin-11 KO mice.<sup>20,23</sup>

Studies of T and NK lymphocytes from the various mutants further illustrated the cumulative functional impact of half-doses of key effectors in the granule-dependent cytotoxicity pathway. The observed reduction in the number of cytotoxic granules stably docking at the immune synapse suggests that both *Rab27a* and syntaxin-11 mediate key steps in granule exocytosis that precede fusion of the granule with the plasma membrane.<sup>1</sup> Although *Rab27a* and syntaxin-11 do not interact directly, the accumulation of limiting effects at distinct steps has a significant impact on overall function. In vivo, the cumulative impact of the partial genetic defects in the granule-dependent cytotoxicity pathway was also manifest when observing the activity of NK cells and the clearance of LCMV.

It is important to note that two major clinical and biological differences between mice with homozygous mutations and mice with combinations of heterozygous mutations were observed. Firstly, although doubly and even triply heterozygous mutants can clear LCMV, a certain proportion of the animal died postinfection. In contrast, homozygous *Stx11*<sup>-/-</sup> mice do not clear the LCMV but always survive.<sup>18,20</sup> Weaker disease progression in *Stx11*<sup>-/-</sup> mice was related to exhaustion of *Stx11*-deficient T cells,<sup>18</sup> ie, a protective process that may not occur in heterozygous mutants. Secondly, circulating WBC counts, and especially T-lymphocyte counts, were elevated 2 weeks after LCMV infection in doubly or triply heterozygous mutants but not in homozygous mutants. This could be related to partial effectiveness of LCMV clearance by residual T-cell cytotoxicity. In the doubly or triply mutants, elimination of the virus likely protects from T-cell exhaustion and therefore not from T-cell–related immunopathology. Thus, in the context of LCMV infection, the intensity of the lymphocytes' cytotoxic response must be balanced between clearance of the virus on one hand and protection against immunopathology driven by excessive T-cell activation on the other hand.

The present study shows that an accumulation of half-doses of key effector molecules in the granule-dependent cytotoxicity pathway creates quantitative traits and prompts qualitative changes in cell behavior. When the accumulation of heterozygous gene mutations exceeds a certain threshold, as in the triply heterozygous ASP mice, HLH immunopathology occurs. This sensitivity to gene dosage has several implications for human disease. Firstly, the cumulative effects of mutations in different genes may characterize the genetic predisposition to rare diseases such as HLH, and might account for “secondary” forms of this syndrome. Some monoallelic mutations may also potentially act in a dominant-negative manner.<sup>39</sup> It is probably too early to be able to appreciate the exact relevance of polygenic inheritance in the secondary forms of HLH. Few retrospective studies reported in some patients the presence of deleterious monoallelic mutations in one or two HLH genes, among the few analyzed.<sup>30,40</sup> Besides, there is no evidence of an increase in rare, putatively pathogenic monoallelic variants in HLH-associated genes in secondary HLH patients so far analyzed.<sup>41</sup> Prospective studies analyzing the different HLH-related genes systematically and the combination of the genes' variants in large cohorts of secondary HLH patients, should help in evaluating the contribution of this genetic mechanism in conferring a greater risk in developing HLH.

Secondly, the gene dosage effect suggests that the addition of monoallelic mutations in genes within this pathway, and possibly in other pathways that are involved in inflammatory processes, could increase an individual risk of developing HLH. It is noteworthy that genetic defects in IL-10 and Myd88 were shown to promote disease development in murine models of HLH.<sup>42,43</sup> Such features have not yet been analyzed in humans. The presence of activating mutations in the nucleotide-binding domain of the inflammasome component *NLR4* was recently found to be associated with recurrent HLH in several patients.<sup>44-46</sup> Similarly, hemizygous *XIAP* mutations, which cause an inherited form of HLH in humans, were shown to result in excessive inflammasome activation in mice.<sup>47</sup> The synergistic effects of these and other candidate genes on the occurrence of HLH should be further tested in murine models. Indeed, murine models of HLH are useful tools for evaluating the risk of disease development under defined genetic and environmental conditions. In humans, the nature of the mutation (null vs hypomorphic), the nature and time of exposure to infectious or inflammatory HLH triggers, and the potential existence of underlying immune disease (such as autoimmunity and lymphoma) make it difficult to predict the risk of HLH in a given individual.

Nevertheless, the murine data reported here argue in favor of a polygenic model for the development of secondary HLH. The occasional reports of heterozygous mutations in secondary HLH are consistent with this model.<sup>26,30</sup> Besides HLH immunopathology, a partial decrease in cytotoxicity resulting from the accumulation of heterozygous mutations in HLH genes may predispose to cancers, as reported in patients with biallelic hypomorphic mutations<sup>24,48,49</sup> or recently, in relatives of patients with primary forms of HLH.<sup>50</sup> More generally, the present results indicate that the cumulative effects of several weak alleles within a given pathway or converging pathways may characterize an individual's genetic predisposition to complex diseases.

## Acknowledgments

The authors thank Dr Pablo Vargas for his help in the analysis of TIRF data, as well as Corina Dragu, Elena Marot, Cedrick Pauchard, and Structure Fédérative de Recherche-Imagine Institute's animal and imaging facilities for their assistance.

This work was supported by the French National Institutes of Health and Medical Research (INSERM), the Agence National de la Recherche (ANR) (ANR HLH-Cytotox/ANR-12-BSV1-0020-01), the Histiocytosis Association of America, the European Research

Council (PIDImmune, advanced grant 249816), and the Imagine Foundation. F.E.S. was supported by fellowships from the Association pour la Recherche sur le Cancer, the ANR, and Becas Chile. S.M. was supported by fellowships from the Association pour la Recherche sur le Cancer, the ANR, and the Imagine Foundation.

## Authorship

Contribution: F.E.S. designed, conducted, and analyzed experiments; A.G. performed and analyzed experiments; S.M. designed, conducted, and analyzed experiments; M.G.-T. assisted for TIRF microscopy experiments; G.M. and A.F. discussed data; F.E.S., A.F., and G.d.S.B. wrote the manuscript; and F.E.S. and G.d.S.B. designed and supervised the overall research.

Conflict-of-interest disclosure: The authors declare no competing financial interests.

Correspondence: Geneviève de Saint Basile, INSERM U1163, Imagine Institute, Hôpital Necker-Enfants Malades, F-75015 Paris, France; e-mail: genevieve.de-saint-basile@inserm.fr; and Fernando E. Sepulveda, INSERM U1163, Imagine Institute, Hôpital Necker-Enfants Malades, F-75015 Paris, France; e-mail: fernando.sepulveda@inserm.fr.

## References

- de Saint Basile G, Ménasché G, Fischer A. Molecular mechanisms of biogenesis and exocytosis of cytotoxic granules. *Nat Rev Immunol*. 2010;10(8):568-579.
- Filipovich AH. Hemophagocytic lymphohistiocytosis and other hemophagocytic disorders. *Immunol Allergy Clin North Am*. 2008;28(2):293-313, viii.
- Janka GE. Familial and acquired hemophagocytic lymphohistiocytosis. *Eur J Pediatr*. 2007;166(2):95-109.
- Janka GE. Familial and acquired hemophagocytic lymphohistiocytosis. *Annu Rev Med*. 2012;63:233-246.
- Janka GE, Lehmborg K. Hemophagocytic syndromes—an update. *Blood Rev*. 2014;28(4):135-142.
- Stepp SE, Dufourcq-Lagelouse R, Le Deist F, et al. Perforin gene defects in familial hemophagocytic lymphohistiocytosis. *Science*. 1999;286(5446):1957-1959.
- Feldmann J, Callebaut I, Raposo G, et al. Munc13-4 is essential for cytolytic granules fusion and is mutated in a form of familial hemophagocytic lymphohistiocytosis (FHL3). *Cell*. 2003;115(4):461-473.
- zur Stadt U, Schmidt S, Kasper B, et al. Linkage of familial hemophagocytic lymphohistiocytosis (FHL) type-4 to chromosome 6q24 and identification of mutations in syntaxin 11. *Hum Mol Genet*. 2005;14(6):827-834.
- Côte M, Ménager MM, Burgess A, et al. Munc18-2 deficiency causes familial hemophagocytic lymphohistiocytosis type 5 and impairs cytotoxic granule exocytosis in patient NK cells. *J Clin Invest*. 2009;119(12):3765-3773.
- zur Stadt U, Rohr J, Seifert W, et al. Familial hemophagocytic lymphohistiocytosis type 5 (FHL-5) is caused by mutations in Munc18-2 and impaired binding to syntaxin 11. *Am J Hum Genet*. 2009;85(4):482-492.
- Ménasché G, Pastural E, Feldmann J, et al. Mutations in RAB27A cause Griscelli syndrome associated with haemophagocytic syndrome. *Nat Genet*. 2000;25(2):173-176.
- Nagle DL, Karim MA, Woolf EA, et al. Identification and mutation analysis of the complete gene for Chediak-Higashi syndrome. *Nat Genet*. 1996;14(3):307-311.
- Barbosa MDFS, Nguyen QA, Tchernev VT, et al. Identification of the homologous beige and Chediak-Higashi syndrome genes [published correction appears in *Nature* 1997;385(6611):97]. *Nature*. 1996;382(6588):262-265.
- Tangye SG. XLP: clinical features and molecular etiology due to mutations in SH2D1A encoding SAP. *J Clin Immunol*. 2014;34(7):772-779.
- Jessen B, Bode SF, Ammann S, et al. The risk of hemophagocytic lymphohistiocytosis in Hermansky-Pudlak syndrome type 2. *Blood*. 2013;121(15):2943-2951.
- Crozat K, Hoebé K, Ugolini S, et al. Jinx, an MCMV susceptibility phenotype caused by disruption of Unc13d: a mouse model of type 3 familial hemophagocytic lymphohistiocytosis. *J Exp Med*. 2007;204(4):853-863.
- Jessen B, Maul-Pavicic A, Ufheil H, et al. Subtle differences in CTL cytotoxicity determine susceptibility to hemophagocytic lymphohistiocytosis in mice and humans with Chediak-Higashi syndrome. *Blood*. 2011;118(17):4620-4629.
- Kögl T, Müller J, Jessen B, et al. Hemophagocytic lymphohistiocytosis in syntaxin-11-deficient mice: T-cell exhaustion limits fatal disease. *Blood*. 2013;121(4):604-613.
- Pachlponik Schmid J, Ho CH, Diana J, et al. A Griscelli syndrome type 2 murine model of hemophagocytic lymphohistiocytosis (HLH). *Eur J Immunol*. 2008;38(11):3219-3225.
- Sepulveda FE, Debeurme F, Ménasché G, et al. Distinct severity of HLH in both human and murine mutants with complete loss of cytotoxic effector PRF1, RAB27A, and STX11. *Blood*. 2013;121(4):595-603.
- Terrell CE, Jordan MB. Perforin deficiency impairs a critical immunoregulatory loop involving murine CD8<sup>+</sup> T cells and dendritic cells. *Blood*. 2013;121(26):5184-5191.
- Sepulveda FE, Maschalidi S, Vosshenrich CA, et al. A novel immunoregulatory role for NK-cell cytotoxicity in protection from HLH-like immunopathology in mice. *Blood*. 2015;125(9):1427-1434.
- Jessen B, Kögl T, Sepulveda FE, de Saint Basile G, Aichele P, Ehl S. Graded defects in cytotoxicity determine severity of hemophagocytic lymphohistiocytosis in humans and mice. *Front Immunol*. 2013;4:448.
- Nagafuji K, Nonami A, Kumano T, et al. Perforin gene mutations in adult-onset hemophagocytic lymphohistiocytosis. *Haematologica*. 2007;92(7):978-981.
- Voskoboinik I, Smyth MJ, Trapani JA. Perforin-mediated target-cell death and immune homeostasis. *Nat Rev Immunol*. 2006;6(12):940-952.
- Zhang K, Jordan MB, Marsh RA, et al. Hypomorphic mutations in PRF1, MUNC13-4, and STXBP2 are associated with adult-onset familial HLH. *Blood*. 2011;118(22):5794-5798.
- Page J, Beutel K, Lehmborg K, et al. Distinct mutations in STXBP2 are associated with variable clinical presentations in patients with familial hemophagocytic lymphohistiocytosis type 5 (FHL5). *Blood*. 2012;119(25):6016-6024.
- Shabbir M, Lucas J, Lazarchick J, Shirai K. Secondary hemophagocytic syndrome in adults: a case series of 18 patients in a single institution and a review of literature. *Hematol Oncol*. 2011;29(2):100-106.
- Zhang M, Behrens EM, Atkinson TP, Shakoory B, Grom AA, Cron RQ. Genetic defects in cytotoxicity in macrophage activation syndrome. *Curr Rheumatol Rep*. 2014;16(9):439.
- Zhang K, Chandrakasan S, Chapman H, et al. Synergistic defects of different molecules in the cytotoxic pathway lead to clinical familial hemophagocytic lymphohistiocytosis. *Blood*. 2014;124(8):1331-1334.



31. Pachlopnik Schmid J, Ho CH, Chrétien F, et al. Neutralization of IFN $\gamma$  defeats haemophagocytosis in LCMV-infected perforin- and Rab27a-deficient mice. *EMBO Mol Med*. 2009;1(2):112-124.
32. Sepulveda FE, Burgess A, Heiligenstein X, et al. LYST controls the biogenesis of the endosomal compartment required for secretory lysosome function. *Traffic*. 2015;16(2):191-203.
33. Jordan MB, Hildeman D, Kappler J, Marrack P. An animal model of hemophagocytic lymphohistiocytosis (HLH): CD8 $^{+}$  T cells and interferon gamma are essential for the disorder. *Blood*. 2004;104(3):735-743.
34. Ahmed R, Salmi A, Butler LD, Chiller JM, Oldstone MB. Selection of genetic variants of lymphocytic choriomeningitis virus in spleens of persistently infected mice. Role in suppression of cytotoxic T lymphocyte response and viral persistence. *J Exp Med*. 1984;160(2):521-540.
35. Waggoner SN, Cornberg M, Selin LK, Welsh RM. Natural killer cells act as rheostats modulating antiviral T cells. *Nature*. 2012;481(7381):394-398.
36. Lang PA, Lang KS, Xu HC, et al. Natural killer cell activation enhances immune pathology and promotes chronic infection by limiting CD8 $^{+}$  T-cell immunity. *Proc Natl Acad Sci USA*. 2012;109(4):1210-1215.
37. Risma K, Jordan MB. Hemophagocytic lymphohistiocytosis: updates and evolving concepts. *Curr Opin Pediatr*. 2012;24(1):9-15.
38. de Saint Basile G, Sepulveda FE, Maschalidi S, Fischer A. Cytotoxic granule secretion by lymphocytes and its link to immune homeostasis. *F1000Res*. 2015;4(F1000 Faculty Rev):930.
39. Spessott WA, Sanmillan ML, McCormick ME, et al. Hemophagocytic lymphohistiocytosis caused by dominant-negative mutations in STXBP2 that inhibit SNARE-mediated membrane fusion. *Blood*. 2015;125(10):1566-1577.
40. Zhang K, Johnson JA, Birochak J, et al. Familial haemophagocytic lymphohistiocytosis in patients who are heterozygous for the A91V perforin variation is often associated with other genetic defects. *Int J Immunogenet*. 2007;34(4):231-233.
41. Tesi B, Lagerstedt-Robinson K, Chiang SC, et al. Targeted high-throughput sequencing for genetic diagnostics of hemophagocytic lymphohistiocytosis. *Genome Med*. 2015;7(1):130.
42. Krebs P, Crozat K, Popkin D, Oldstone MB, Beutler B. Disruption of MyD88 signaling suppresses hemophagocytic lymphohistiocytosis in mice. *Blood*. 2011;117(24):6582-6588.
43. Behrens EM, Canna SW, Slade K, et al. Repeated TLR9 stimulation results in macrophage activation syndrome-like disease in mice. *J Clin Invest*. 2011;121(6):2264-2277.
44. Romberg N, Al Moussawi K, Nelson-Williams C, et al. Mutation of NLRP4 causes a syndrome of enterocolitis and autoinflammation. *Nat Genet*. 2014;46(10):1135-1139.
45. Canna SW, de Jesus AA, Gouni S, et al. An activating NLRP4 inflammasome mutation causes autoinflammation with recurrent macrophage activation syndrome. *Nat Genet*. 2014;46(10):1140-1146.
46. Kitamura A, Sasaki Y, Abe T, Kano H, Yasutomo K. An inherited mutation in NLRP4 causes autoinflammation in human and mice. *J Exp Med*. 2014;211(12):2385-2396.
47. Yabal M, Müller N, Adler H, et al. XIAP restricts TNF- and RIP3-dependent cell death and inflammasome activation. *Cell Reports*. 2014;7(6):1796-1808.
48. Chia J, Yeo KP, Whisstock JC, Dunstone MA, Trapani JA, Voskoboinik I. Temperature sensitivity of human perforin mutants unmasks subtotal loss of cytotoxicity, delayed FHL, and a predisposition to cancer. *Proc Natl Acad Sci USA*. 2009;106(24):9809-9814.
49. Mancebo E, Allende LM, Guzmán M, et al. Familial hemophagocytic lymphohistiocytosis in an adult patient homozygous for A91V in the perforin gene, with tuberculosis infection. *Haematologica*. 2006;91(9):1257-1260.
50. Löfstedt A, Chiang SC, Onelöv E, Bryceson YT, Meeths M, Henter JL. Cancer risk in relatives of patients with a primary disorder of lymphocyte cytotoxicity: a retrospective cohort study. *Lancet Haematol*. 2015;2(12):e536-e542.